

Accepted Manuscript

Seismic Behavior of Under Confined Square Reinforced Concrete Columns

Aditya Singh Rajput, Umesh Kumar Sharma



PII: S2352-0124(17)30070-X
DOI: doi:[10.1016/j.istruc.2017.10.005](https://doi.org/10.1016/j.istruc.2017.10.005)
Reference: ISTRUC 232
To appear in: *Structures*
Received date: 30 June 2017
Revised date: 26 September 2017
Accepted date: 29 October 2017

Please cite this article as: Aditya Singh Rajput, Umesh Kumar Sharma , Seismic Behavior of Under Confined Square Reinforced Concrete Columns. The address for the corresponding author was captured as affiliation for all authors. Please check if appropriate. Istruc(2017), doi:[10.1016/j.istruc.2017.10.005](https://doi.org/10.1016/j.istruc.2017.10.005)

This is a PDF file of an unedited manuscript that has been accepted for publication. As a service to our customers we are providing this early version of the manuscript. The manuscript will undergo copyediting, typesetting, and review of the resulting proof before it is published in its final form. Please note that during the production process errors may be discovered which could affect the content, and all legal disclaimers that apply to the journal pertain.

SEISMIC BEHAVIOUR OF UNDER CONFINED SQUARE REINFORCED CONCRETE COLUMNS

Author-1 (Also, Corresponding Author)

Name: - Aditya Singh Rajput.
Qualification: - M-Tech, Ph.D. (Pursuing).
Current Designation: - Research Scholar.
Organization: - Indian Institute of Technology, Roorkee.
Email ID: - adirajcivil@gmail.com
Contact Number: - +91-8266803773.
Address: - F-109, Azad Bhawan, IIT Roorkee, 247667, India.

Author-2

Name: - Dr. Umesh Kumar Sharma.
Qualification: - Ph.D.
Current Designation: - Associate Professor.
Organization: - Indian Institute of Technology, Roorkee.
Email ID: - umuksh@radiffmail.com
Contact Number: - +91-9359050255.
Address: - 133, Civil Engineering Department, IIT Roorkee, 247667, India.

ABSTRACT

The role of confining reinforcement in dissipating a large amount of energy in reinforced concrete (RC) elements at the time of seismic events has been well demonstrated in previous studies. In India, this practice of providing special confinement in RC elements began to be followed after the ductile detailing code came into being in the year 1993. Hence, the structures built before 1990s in seismically active areas had no ductile detailing, as the design recommendation of pre 90s era do not consider adequate confinement requirements. The Present experimental study is a part of an ongoing project of upgrading these old reinforced concrete structures, which had no special confinement and are located in seismically active regions. Three full-scale columns with different amount of transverse reinforcement (volumetric ratio of 1.31, 0.33, and 0.22) were tested in a specially made testing setup. One specimen was designed as per the current Indian guidelines for ductile detailing (IS 13920:2016), while the other two specimens were designed as per the guidelines which existed before the Code on ductile detailing was implemented. The response of the columns under quasi-static reverse lateral cyclic loading (at constant axial load) was recorded in terms of lateral load v/s deflection, moment v/s curvature, energy dissipation, stiffness reduction and different ductility parameters. As expected, the results of the study show inferior seismic performance of under-confined columns as indicated by the key strength and ductility parameters. The results have though quantified the strength and ductility deficit of these under confined RC columns, which shall be of great help in designing suitable retrofit for the existing structures constructed with no ductile detailing features.

INTRODUCTION

The ability of columns to absorb a large amount of energy during a seismic event plays a vital role in defining the seismic response and stability of a structure [1-2]. Provisions of providing special confining reinforcement in the plastic hinge regions have emerged as one of the methods for ensuring the ductile performance [3-6]. But the provisions of ductile detailing were introduced in India in the early 90s [3], and the structures built before this period lack these detailing features. Further, more than fifty percent of Indian land is prone to the earthquakes (land under seismic zones – III, IV and V). The Himalayan-Naga lushai region, Indo-Gangetic plain, North- East region of India, Western India, Kutch and Kathiawar regions are seismically

active regions. Several past seismic events have highlighted the inadequacy of the structures in different forms. Latur earthquake 1993 (8000 deaths), 1997 Jabalpur earthquake (38 deaths), 1999 Chamoli earthquake (100 deaths), 2001 Gujarat Earthquake (18000 deaths), 2005 Kashmir earthquake (70,000), Nepal earthquake (9000 deaths) etc. are the prominent examples. One of the key reasons behind these disastrous consequences was inadequate transverse reinforcement confinement in the plastic hinge regions of the columns [7]. This demands immediate quantification of deficiency of transverse reinforcement in the potential plastic hinge regions of RC columns and thereby to devise suitable upgrading of the under confined columns. Towards this end this study attempts to ascertain the deficiency of RC columns that have no special confining reinforcement in the end hinge regions. Three full-scale columns were tested in accordance with the testing protocol suggested by the ACI guidelines [8].

SIGNIFICANCE OF RESEARCH

Reinforced concrete columns are the vital elements of structural systems to transfer gravity as well as lateral loads; hence it is expected for the columns to yield superior performance. Though, efforts for improving structural performance of columns started in late 19th century, pioneer work of Richart et al. (1929) substantially improved the knowledge and understanding about the role of confinement in RC columns. In the middle two quarters of 20th century, substantial experimental and analytical work was reported highlighting influences of different parameters of confinement of RC columns. Study reported by Sheikh [9] compiles these previous studies in a very elaborate manner. Experimental and analytical investigations of large-scale RC columns received significant attentions of the researcher in last quarter of 20th century. Prominent work in this context started in early 60s [10], wherein it was concluded that the level of axial force available during the reversal of lateral loading had a significant influence over column's seismic response. Further studies in this context conducted in different parts of world investigated different parameters which included loading regimes [11], presence of footing/stub [12], effect of concrete grades [13], influence of transverse reinforcement [14], [15], and influence of axial load variations [16]. The updated design guidelines to account for extended scope of transverse reinforcement (as effective confining reinforcement) have been introduced in different parts of world in last two decades of 20th century. However, all the previous studies mainly talked about the importance of confinement and reported their test data with an aim to construct new well designed confined concrete columns against seismic actions. Their aim was not to report the

structural deficiencies in the under-confined or unconfined concrete columns in order to retrofit such columns. The truth of the matter is that there are many columns which are deficient and are in urgent need of confinement up gradation. Thus a careful well designed retrofit is often required to upgrade such deficient building columns. In order to design a retrofit, all the key structural properties of the deficient under confined sections of the RC elements are generally required. In view of the above this paper presents various structural properties of under confined columns for enabling their proper seismic retrofit.

Presently, seismic design practices are noticeable drifting toward performance based design. This approach enables the building to attain predicted performance levels during the seismic events. This objective of predefined performance may be achieved by enabling the building components (beam, columns, joints and slabs) to mobilize targeted performance levels. Present study examined the seismic performance level of RC columns by evaluating useful performance indices (curvature ductility and displacement ductility). Also, this study examines different useful response parameters and compares the results with the existing studies to generate a better understanding. Despite the fact that a good number of studies in similar context has been reported, studies giving performance indices are very scarce. Recently published document by ACI committee [8] in 2013 explicitly underlines the requirement of such studied which involve determining performance indices using state of the art knowledge. Further, Due to the increased interest in performance based design, various retrofitting techniques have been developed and designed taking ductility factors as input parameters [17]. Also, recently published seismic strengthening guideline ACI 440.2R-2017 [18] takes ductility demand as input parameter for designing external retrofit for deficient columns (Ch-13). Since, detailed studies in this context providing performance indices (especially curvature demand) for differently configured RC columns are scarcely available, it is believed that the data from the present study shall help designers to design seismic retrofit towards this end.

SPECIMEN PREPARATION

Three column specimens, each of height 1800 mm and cross section 300 x 300 mm, were constructed along with a stub of size 1000x600x500 (Figure 1). The specimens UC1 and UC2 represented the columns of a RC building frame or bridge with inadequate transverse confining reinforcement, while the specimen D-1 was designed in accordance with the current ductile

detailing code with transverse reinforcement ratio as 1.31% i.e. stirrup spacing of 75mm [3]. The underconfined specimens UC1 and UC2 were designed according to the pre ductile detailing code era [19] with reinforcement ratios 0.33 and 0.22 respectively represented by stirrup spacing of 300mm. While the specimen UC2 had only perimeter tie, the UC1 had cross ties in addition to perimeter tie. Both UC1 and UC2 though satisfied the pre IS: 13920-1993 [20] era, but violated the current code requirements as the spacing of ties was 300 mm. Table 1 provides the key details of the specimens. Thus the main variable of the study was amount of confining reinforcement (identified by the stirrup spacing and stirrup configuration) as shown in Figure 1.

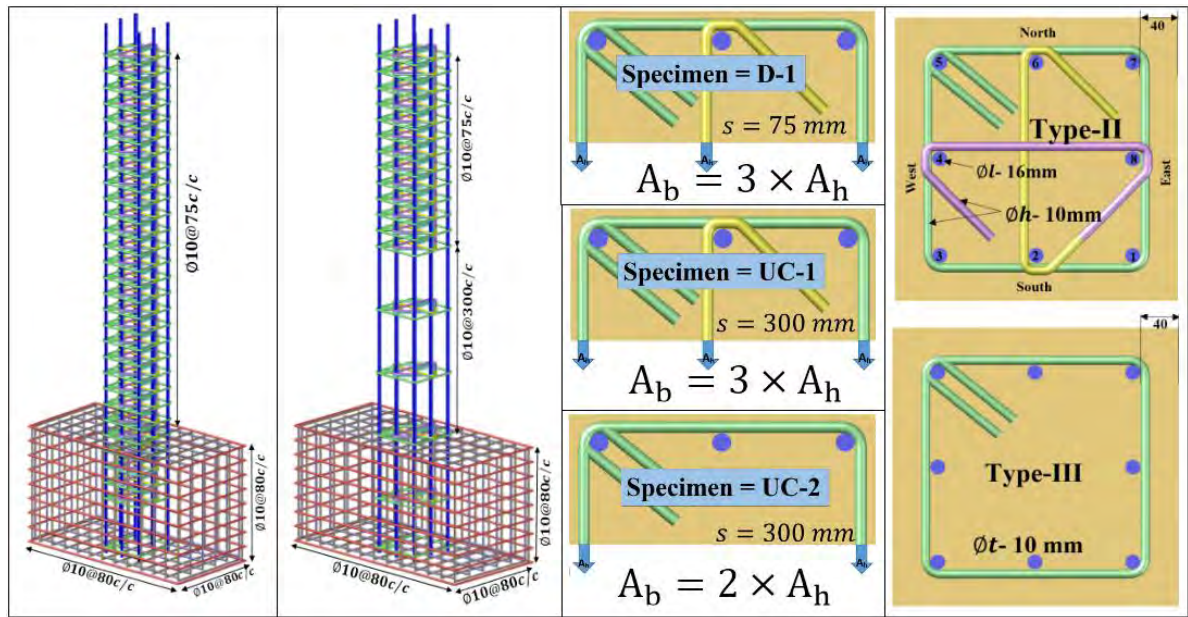


Figure 1:- Reinforcement Details of Specimens D-1, UC-1, and UC-2.

The design of concrete mix was done according to the current Indian guidelines [21] for the specimen D-1 and as per old Indian guidelines (IS-456:1964) for specimen UC-1 and UC-2. Six companion cubes and cylinders were cast with each column specimen. Three cubes and three cylinders were tested after 28 days of casting to determine the concrete strength, while three cubes and cylinders were tested to measure the strength of concrete on the day of testing of the full-scale specimens. This cylinder concrete strength (f'_c) was used in calculating the amount of axial load to be maintained on the column during testing. An axial load (P) of $0.33P_0$ was applied on all the specimens during lateral cyclic testing.

Where, $P = 0.85 \times f'_c \times A_c + f_y \times A_{st}$ Equation

1

The axial load levels in this testing represents the dead or gravity loads in column at the time of seismic event. Studies in the past have taken different load levels (ranging from 0.1 to 0.7) based on different considerations. In the present study, reason behind selecting this factor of 0.33/0.35 was the results of some buildings analyzed in the SAP-2000 (Structural analysis program). These buildings were of three to four stories, and the dead loads of the ground story columns were recorded. These gravity load levels in the analysis was ranging in between $0.3P_0$ to $0.4P_0$, and hence a factor of 0.33/0.35 was taken.

Specimens were prepared in a vertical mold made up of two parts namely footing part and column portion. The provision was made for accommodating eight tie rods in the footing area to facilitate connection of footing with the strong girder floor at the time of testing. An arrangement using a slit and blade system was prepared to facilitate through bars on the test length of 700mm from stub column interface. This test length represented end potential hinge regions of columns. Through rods were provided to attach LVDT's in the test length to record flexural rotation and shear distortion during the testing. Strain gauges were also pasted on reinforcement to record strains at various critical locations. Rotating drum mixture and needle vibrator were used for casting the specimens. Specimens were cured using wet gunny bags for 28 days and then kept under laboratory ambient conditions until the day of testing which was 60 days after casting.

Table 1: - Details of specimens.

Specimen ID	Tie Spacing	Tie	f'_c (MPa)	A_b (mm^2)	$A_{sh(\text{req})}$ (mm^2)	$A_{sh(\text{Provided})}$ (mm^2)	A_{shp}/A_{shr}	$\rho_{sh} = \frac{A_{sh}}{s.b_c} \times 100$
D-1	75	II	32.74	75π	54.67	78.54	1.44	1.31
UC-1	300	II	32.34	75π	145.8	78.54	0.54	0.33
UC-2	300	III	33.40	50π	269.68	78.54	0.29	0.22

LATERAL LOAD HISTORY DESIGN

The specimens were tested under lateral cyclic loading in a quasi-static manner. Cracked section analysis in SAP-2000 (structural analysis program) for lateral load vs. deflection

produced yield deflection as 15.678 mm \approx 15mm, yield drift ratio of 0.01 or 1% and yield lateral load as 83.7 kN (Figure 2).

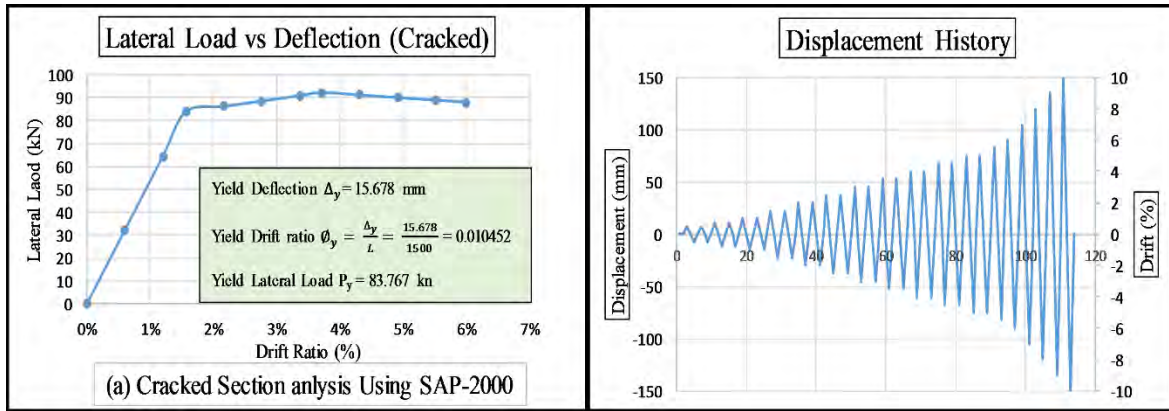


Figure 2: - Design of lateral displacement history

Based on these results and taking into consideration the recommendations of the ACI 374.2R-13 [8], lateral load history was designed with two cycle loading each up to 5% drift and single cycle after 5% drift (Figure 2).

INSTRUMENTATION

A robust instrumentation was employed in order to record maximum response parameters of the column during testing. A total of 31 LVDT's were used to measure longitudinal deflections, curvature values, slip of column, transverse deflections, shear distortion and footing movements (Figure 3). Twenty strain gauges were attached to the reinforcement of columns in order to record strain values of critical locations in reinforcement. Two load cells were used to record load values in longitudinal and transverse directions. A hydraulic jack of 400-ton capacity was used to apply axial compression on the column and an actuator of 50-ton capacity with \pm 300mm travel length was employed for slow lateral cyclic loading. All the data were recorded with the help of signal conditioner and data-taker, and stored in the computer.

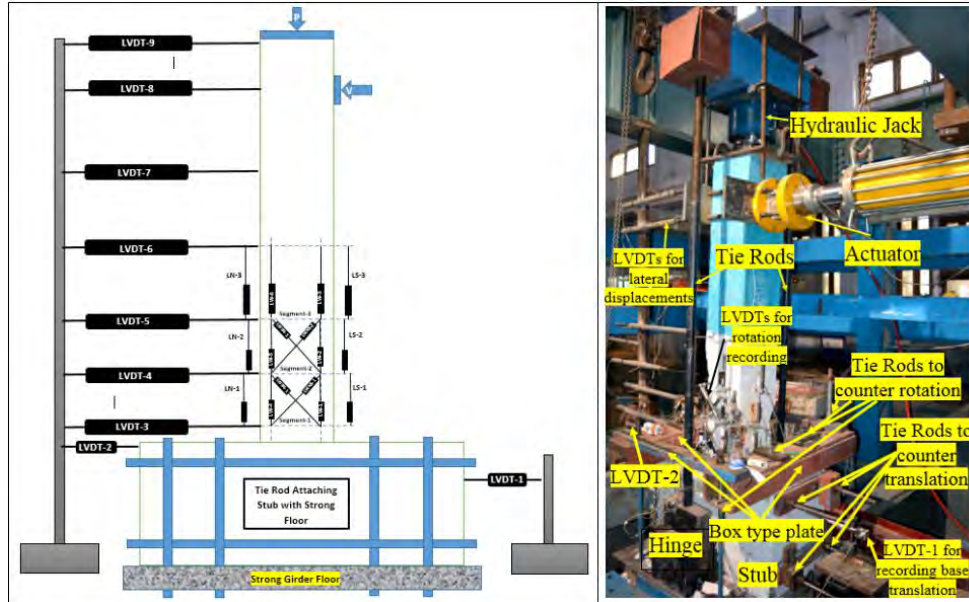


Figure 3: - Schematic Diagram of column testing setup and instrumentation

TESTING

Specimens were tested in a specially fabricated setup to simulate seismic loading conditions (Figure 3). After fixing the base with strong floor using 12 tie rods, sensors (LVDTs, load cells, and strain gauges) were attached to data acquisition system using data logger. Testing started with the application of axial load (simulating gravity load) first. The concentricity of the axial load was ensured by making the appropriate adjustments in the contact area of jack and columns interface. The readings of strain gauges and LVDTs were also used to monitor concentricity of axial load. After ensuring the concentricity, the axial load was applied in a steps (increment of 200 kN) to avoid any local failure of the system or specimen. The rate of axial loading was kept as 25kN/minute approximately. Application of quasi-static lateral loading started after half an hour of applying the full axial load. Rate of lateral cyclic loading, which was in terms of displacement control manner, was kept very low (0.05mm/sec) to avoid any inertial force effect or strain rate effect. In the lateral displacement excursion, each increment consisted of two cycles with a drift increment of 0.5% until 5% drift level. After this drift level one cycle increment of similar drift ratio was applied. The progress of test was monitored and damage of specimens in terms of crack propagation was recorded using a crack scope with an accuracy of 0.02mm. Damage history was monitored at peak of each cycle and these observations have been reported in the subsequent part.

RESULTS AND DISCUSSION

Three specimens with different amount of transverse confining reinforcement were tested under quasi-static lateral cyclic loading in this study. The observations of damage during the testing and other key parameters of strength and deformability evaluation were used in comparing the structural performance of the various specimens. Authors in the past have defined different limits for termination of such tests. Ohno et al. [1] used the post-peak behaviour up to yield strength as the point of termination [1][1][1][1][1][1], Sheikh et al. [12] recommended testing up to 20% reduction of lateral load capacity in post peak, and even some other authors have suggested taking gravity load reduction as failure criteria [22]. In this study the tests were continued up to the post-peak point when there was 20% reduction in the peak lateral load. Different performance parameters and response plots were computed to present a clear picture of the seismic performance of these columns.

Observations

The observations during testing in terms of initiation of cracking, propagation of cracks, yielding of reinforcement, crushing of concrete, delamination/spalling of concrete and buckling of reinforcement were recorded during simulated seismic testing. As expected the control column specimen D1 responded in a ductile manner as compared to under confined columns UC1 and UC2. Initial distress in the specimens occurred in terms of flexural cracking on the south and north faces (flexural faces). It was observed that though the column section at the stub column interface was subjected to maximum moment, damage in the initial cycles was marked away from this section (Figure 4). The distance of initial failure region from the stub-column interface varied in the test specimens with in a portion of $2d$ (600mm in present study). This observation has also been made in some previous studies [23]. The reason behind this response was the mobilization of extra confinement in the near stub sections due to the presence of significant axial load.

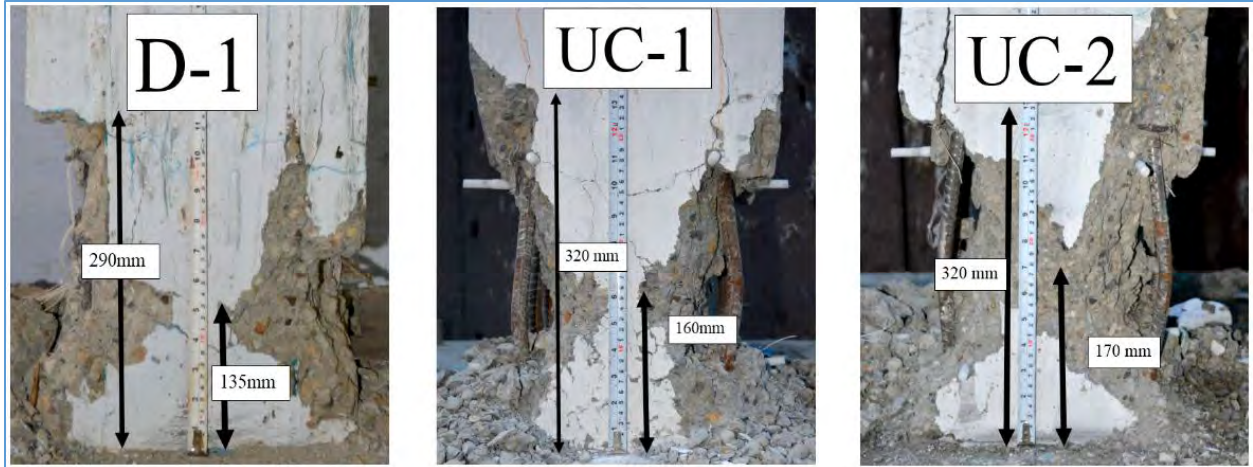


Figure 4:- Damaged specimens after testing (Hinging portion)

First crack in the specimens appeared at 0.75% drift at a distance of 470mm, 280mm and 260 mm from the stub face in specimens D1, UC1 and UC2 respectively. This initial Crack width was measured to be 0.02 mm in D1 specimen and about 0.04 mm in under-confined UC1 and UC2 specimens. In further lateral load excursions, cracks in the flexural faces (south and north) developed and widening of cracks was observed. The width of crack at 1% drift was 0.06mm, 0.08 and 0.1 mm in specimens D1, UC1 and UC2 respectively and these cracks further widened to 0.46, 0.8 and 1 mm as the drift increased to 3.5%. The extent of damaged portions spread to around 300 mm to 400 mm in all the specimens with central distance of the damaged regions from stub interface being 135, 160 and 170 mm for the specimens D1, UC1, and UC2 respectively. Buckling of the longitudinal reinforcement bar was observed as the primary reason of final failure (Figure 4). During the higher lateral load excursions the already formed flexural cracks also propagated to the other side faces at an inclination angles of 30° to 45° . It should be noted that the crack width also varied along the length of the crack. Hence a point was marked in each crack and it was monitored to measure the increase in width to gauge the relative development in crack width. Increase in crack width was monitored on tension face at the peak of each cycle. The rapid propagation and increase in width of crack in specimens UC1 and UC2 indicated inability of these specimens in controlling cracks whereas, well confined D1 column showed good control over crack widening. Figure 6 shows the crack propagation plots of specimens at different drift levels.

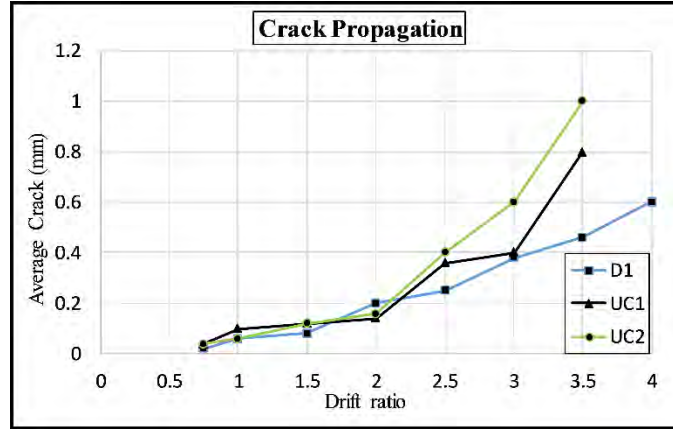


Figure 5: - Crack propagation plot corresponding to different drift levels.

It should be noted that the ability to sustain gravity loads even after large lateral load excursions is one very important indicator for ensuring structural stability and hence observing axial load reduction at progressing drift levels was one important observation of present study. Gravity collapse has been considered as an important failure stage in different studies [24]. Columns performance against gravity load and lateral loads has been studied [25] and the results has been interpreted the effect of different parameters [22]. A study by Nakamura and Yoshimura (2014) [26] has also concluded that reduction in the axial load after significant damage results to increases in the collapse drift up to two to six times. In present study the axial load was applied prior to the application of lateral loading, and then the reduction in the axial loads after each drift cycle was monitored. Figure 6 shows the reduction in the axial load after every applied drift. It can be observed that the ductile column specimen D1 sustained gravity load till large lateral flexural cycles and experienced only 13% reduction in gravity load at 6% drift. Whereas the specimens UC1 and UC2 showed inferior behavior in sustaining the gravity load during the lateral cyclic loading. The reason behind this behavior of UC1 and UC2 specimens is because of widely spaced ties resulting into buckling of longitudinal bars. Further, it was noted that the specimen UC2 behaved similar to UC1 in initial cycles but after 3.5% drift the reduction in axial load in specimen UC2 was more rapid as compared to UC1. This is due to the inferior configuration of transverse ties in UC2 compared to that in UC1.

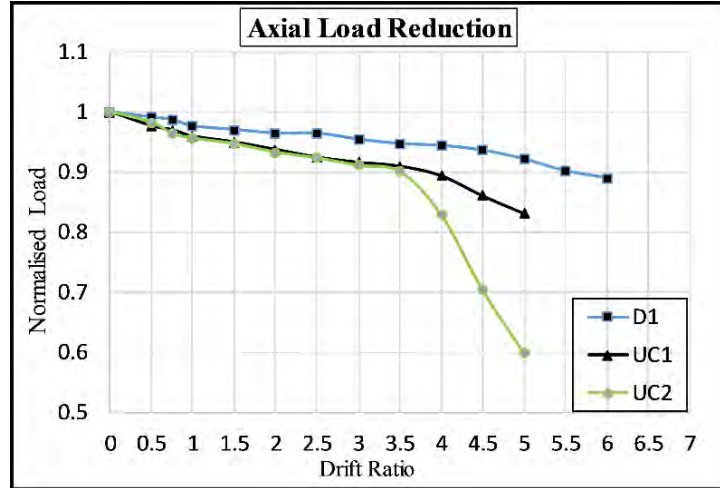


Figure 6:- Axial load reduction at increasing drifts.

Lateral Load v/s Deflection Response

The response of column specimens was measured in terms of lateral load and the corresponding deflection (V - δ). The lateral load (V) was captured using a ± 500 kN load cell attached to the actuator and the corresponding lateral deflection (δ) of loading point was recorded using LVDT located at the load point. Figure 7 a-c shows the V - δ responses for all the three specimens along with their backbone curves. Figure 7 (d) presents a comparison of backbone curves of the three specimens. Important stages like initiation of crack, concrete crushing and reinforcement buckling have been marked on the plots to provide better description. Though the aim was to terminate the test when a reduction of 20% in lateral load is reached in the post-peak side, the test was continued even after that, wherever possible, in order to capture the post peak behaviour at larger lateral displacements and to monitor the reduction in gravity load sustaining capacity. Unfortunately, the test had to be terminated slightly early in D1 specimen due to some technical problem in actuator and the entire targeted post-peak portion could not be captured.

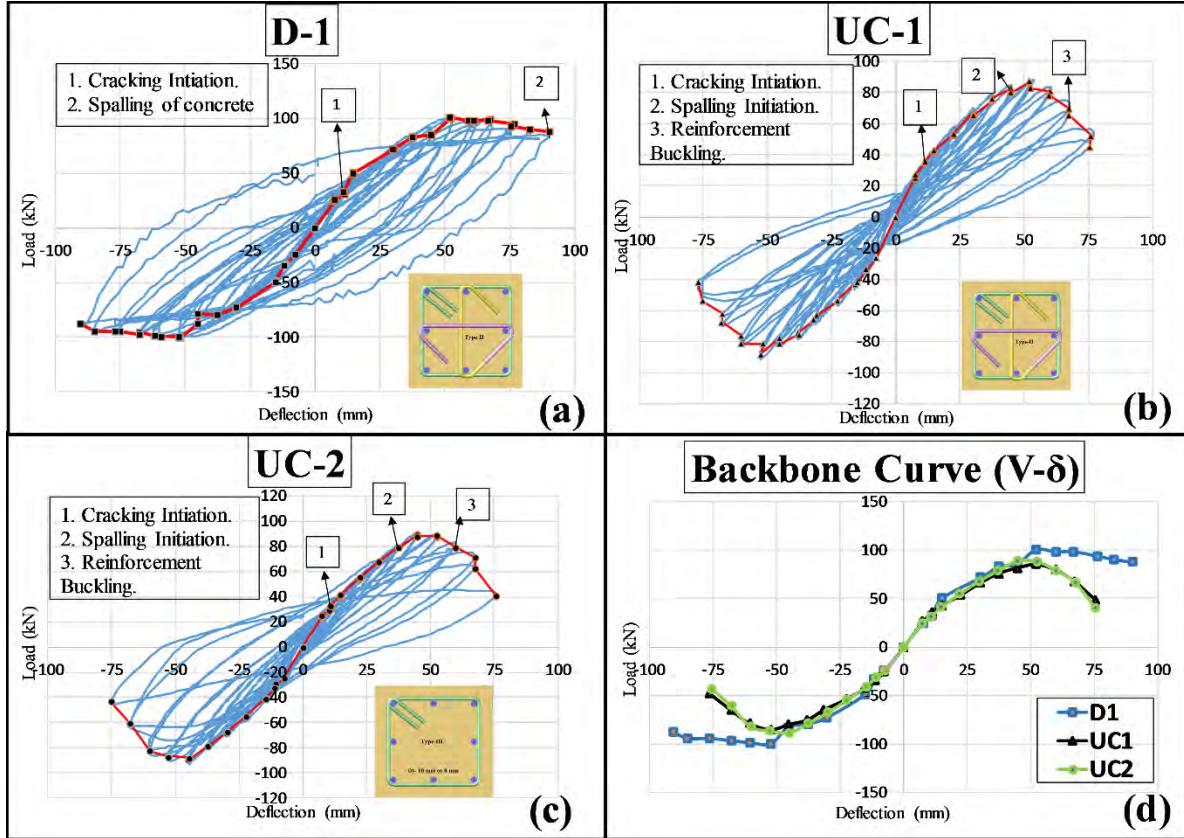


Figure 7: - Lateral load v/s Lateral deflection plots of specimens.

Moment v/s Curvature Relationships

Moment-curvature relationships were also computed for the specimens from the measured data. Towards this end, the test length of the columns was divided into three segments as shown earlier in Figure 3. In each segment, six LVDTs were attached in the longitudinal direction using through rods to record flexural rotation. The LVDTs had special end bearing design which allowed their rotation in both the planes without any obstruction. Previous researches have used two different methodologies of locating LVDTs for measuring displacements in order to determine curvatures. One procedure uses LVDTs being placed on flexural faces (Ls1 and Ln1) [27], while another procedure recommends fixing LVDTs on the side faces (Lw1 and Lw4) [13]. Since no effective comparison between these two methodologies was available, both the methods were used to measure displacements and then the curvatures were computed. It was observed from the test results that the methodology involving placement of LVDTs on the side faces provides more effective measurements for curvatures. This may be attributed to the fact that the end points of LVDTs in side face arrangement represent the deflection of confined core in a

more effective way as the holding rods go through the periphery of core. The results presented here are from the side face placement of LVDTs. Though in all the specimens damaged zone was found to spread to 500mm (approximately), segment 1 was the critically damaged portion. Hence in this study, the results of the curvature of segment 1 have been presented. The methodology of calculating experimental curvature has been shown in Figure 8.

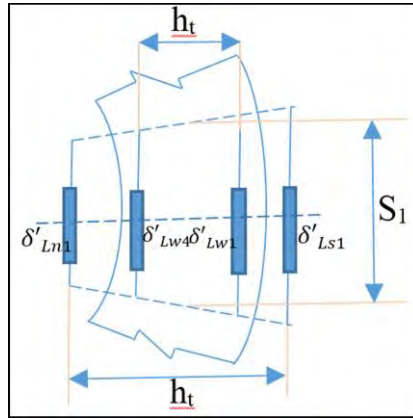


Figure 8: - Measurement and Computation of Curvature

$$\text{Flexural Rotation} - \theta_{s1} = \frac{\delta'_{Ls1} - \delta'_{Ln1}}{h_t} \quad \text{Or} \quad \frac{\delta'_{Lw1} - \delta'_{Lw4}}{h_t} \quad \text{Equation 2}$$

$$\text{Average Curvature} - \phi = \frac{\theta_{f2}}{S_1} \quad \text{Equation 3}$$

Figure 9(a)-(c) presents the M- ϕ behavior of all the three columns and Figure 9 (d) presents a comparison of backbone curves for all the specimens. It should be noted that moment value in these responses includes the components of the primary moment (lateral load) and secondary moment (P- Δ), and the curvature is the average of one segment (critically damaged segment). It is important to observe that the V- δ response of specimens UC1 and UC2 was almost similar but the M- ϕ response of UC2 was inferior to UC1. This is because of reduced P- Δ component in moment value owing to inferior axial load sustaining capability of specimen UC2 due to poor tie configuration. Moment v/s curvature relationships show reduced moments of 19% and 29% for the specimens UC1 and UC2 respectively. Inferior post peak behaviour of under confined specimen highlights the vulnerability of catastrophic failure of these specimens during any seismic event. It can also be said that the M- ϕ response is a better representation of the seismic performance of a column than the V- δ response. The reason being the fact that M- ϕ presents the

sectional level behaviour which is influenced by global parameters like spacing of stirrups, tie arrangement and axial load level etc.

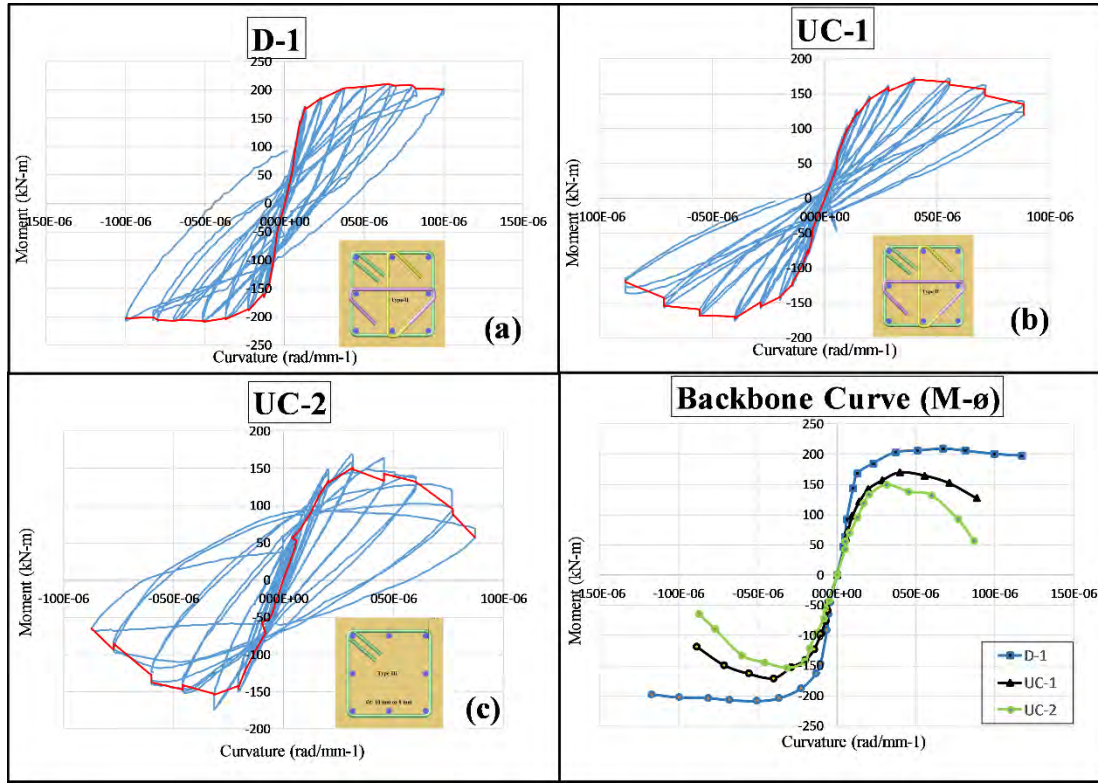


Figure 9: - Moment v/s Curvature response of specimens

Stiffness Degradation

Secant Stiffness (K) of each cycle was calculated using the slope of the lines joining the peaks of negative (K_n^-) and positive (K_n^+) phases as shown in Figure 10(a). Average stiffness (K_n) was calculated for each drift level based on number of repetitive cycles (i.e. two cycles up to 5% drift and then one cycle afterwards). Equations 4 & 5 explain the procedure for this computation. Since the initial stiffness of all specimens was almost similar, normalization was not done and the actual values have been presented in the Figure 10(b).

$$\text{Secant Stiffness} = K_n^+ = \frac{\sum_{i=1}^i V_n^+(\text{max})}{\sum_{i=1}^i \delta_n^+(\text{max})}, \quad K_n^- = \frac{\sum_{i=1}^i V_n^-(\text{max})}{\sum_{i=1}^i \delta_n^-(\text{max})} \quad \text{Equation-4}$$

$$\text{Average Stiffness} = K_n = \frac{K_n^+ + K_n^-}{2} \quad \text{Equation-5}$$

Degradation in the secant stiffness during the loading process with respect to drift ratio has been compared in Figure 10 (b). An almost similar initial stiffness of all the specimens may be attributed to the fact that the stiffness in the initial cycles depends on the health of concrete, which would be similar for all the specimens. It is evident in the response plot (Figure 10 (b)) that, at 5% drift level stiffness of the specimen D1 got reduced to 37% whereas stiffness of specimens UC1 and UC2 reduced to 18.5% and 16.5% level. Similar studies [28] in the past have reported similar trends of more than 80% reduction in the flexural stiffness at higher drift levels. Studies over rectangular and circular testing have also reported significant reduction in the flexural stiffness [29].

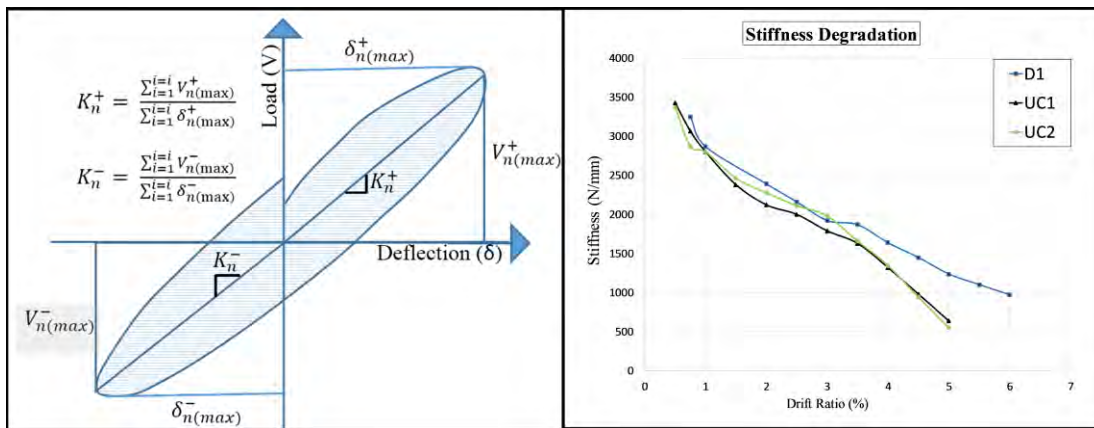


Figure 10: - Stiffness degradation computation and its results for all the specimens.

Cumulative Energy Dissipation

The energy dissipation capacity of any structural element is an important indicator of its energy absorbing capability before failure [30]. Higher energy dissipation capacity is a depiction of superior post peak behavior and a ductile failure. This parameter is mathematically represented as the area under the load v/s deflection curve, and in the case of cyclic loading; it is represented as the effective area within the hysteresis loop (marked as Δ^e in Figure 11). Figure 11 presents the graphical representation of the area within the hysteresis loop (Area ABCDEF). This area was calculated using the MATLAB Code for all the specimens.

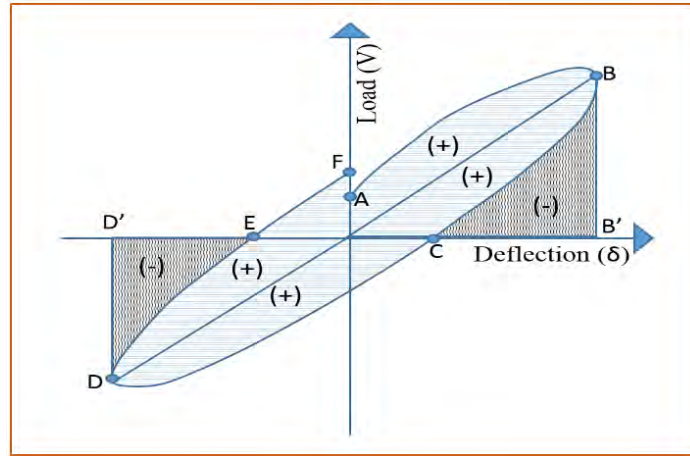


Figure 11:- Schematic of Energy dissipation Computation

Dissipated energy for each cycle was evaluated and averaged according to the number of repetitive cycles. Figure 12(a) presents a quantitative comparison of the dissipated energy at different drift levels, while Figure 12(b) presents the increase in the energy dissipation with increasing displacement demand. It is evident from these responses that despite almost similar behaviour in the beginning for all specimens, the ductile specimen D1 took a significant lead in energy dissipation after 3% drift ratio. This is because of superior strength and post-peak performance of ductile detailed specimen resulting in to a higher area under the hysteresis loop. It should be mentioned here that the response of specimen D1 was only up to 10% load reduction in post peak so even much better energy dissipation could be expected.

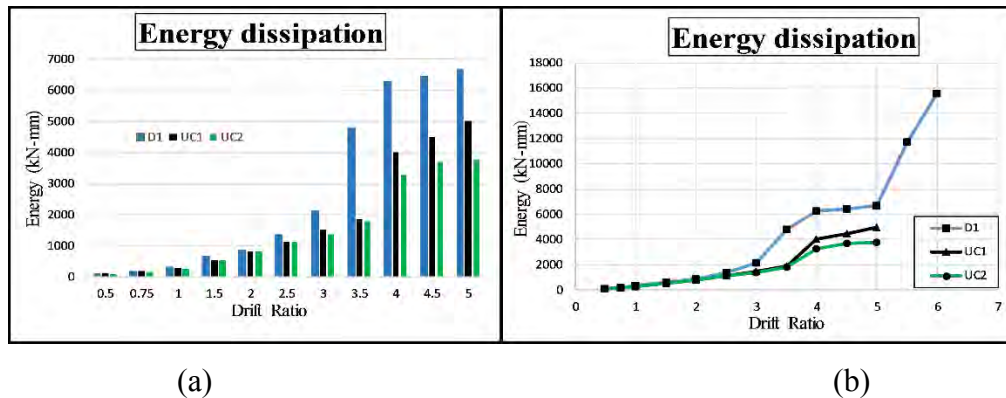


Figure 12: - Energy dissipation results and Variation of Energy Dissipation with drift ratio

Ductility Ratios

Different deformability performance indices (displacement ductility and curvature ductility) were also computed using the response data for better presentation of the seismic performance.

For calculating these indices, envelope curves of all these specimens were drawn by averaging the positive and negative cycles. Figure 13(a) and (b) presents the envelope curves of V- δ and M- ϕ responses respectively and formulation for calculating the performance indices. Yield point of the responses was determined as the intersection point of horizontal line joining the maximum load point value and secant line joining the 65% of maximum value. It should be noted that while the load-displacement plots present the performance of the whole test length of the specimens, the moment-curvature plots present the behaviour of only the critical sections. These indices have been used by different design guidelines worldwide and are termed as performance parameters. New Zealand Standard guidelines [6] take curvature ductility as basic performance parameter whereas Canadian Standard [5] considers displacement ductility as the seismic performance parameter of a RC section. Both the indices were evaluated in the present study using the obtained results and are presented in the Table 2. Other important parameters like cumulative energy dissipation, maximum attained lateral load and maximum achieved moment are also given in Table 2. Results from some previous studies have also been summarized in Table 2 and a comparison in this regard is described in the following sections.

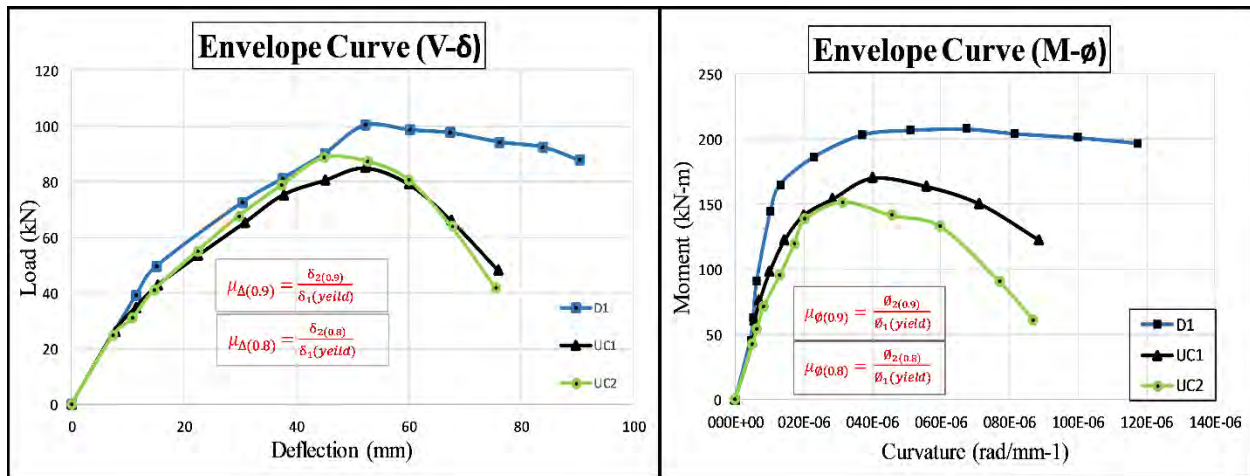


Figure 13: - Envelope curves of hysteresis response of specimens

Previous Studies and Discussion

The existing literature shows that there are many key material and structural parameters which influence the seismic performance of reinforced concrete elements. These parameters for columns are material properties like concrete and reinforcement strength [31], axial load levels [16], [32], reinforcement characteristics like tie spacing, volumetric ratio of tie reinforcement

[14], [15], tie configuration, and amount of longitudinal reinforcement, A_g/A_c [22] etc. Among all these parameters, the transverse confining reinforcement characteristics is believed to be the most important parameter. Table 2 summarizes the seismic performance results from some past studies for stubbed RC square columns with respect to transverse confining steel properties along with the results of this study. It is evident from the present as well as previous studies that the seismic performance of RC columns is significantly affected by the amount of transverse reinforcement. The specimens with higher tie spacing (s) and lower tie (ϕ_h) diameter responded poorly against seismic loading in terms of deformability and strength. Despite similar concrete and longitudinal reinforcement, specimens UC1 and UC2 had reported 13% lower lateral load capacity compared to the well confined D1 specimen which may only be attributed to inadequate confinement in UC1 and UC2 specimens. The results of previous studies and also a comparison of UC1 and UC2 specimens show that configuration of tie confinement is also important as specimen with better configuration i.e. UC1 had better performance than the UC2 specimen which had only perimeter tie. In addition, axial load plots show that the specimen with poorer configuration of transverse reinforcement showed rapid reduction in axial load during lateral load excursion and ultimately resulted in to lower moment capacities. The difference in moment capacities of UC1 and UC2 indicates the fact that inferior configuration (not supporting all the longitudinal bars) affects the M v/s δ behavior more severely than V - δ response. A perusal of performance indices given in Table 2 presents a clear picture of key seismic indices. Lower values of these indices point towards a need of significant improvement with respect to various parameters of confinement and also minimum ductility demand parameters. It is given in the current recommendations in various international standards to set the lower limit of displacement ductility as 4 [CSA A23.3] and curvature ductility as 20 [NZS:3101]. Thus quantifying deficiencies in under confined columns and understanding ductility performance demands is important for the seismic retrofit of RC columns which are part of the structures built before the ductile detailing codes came into being. Term $\mu\delta$ (0.9) stands for deflection corresponding to load level when V_{max} reduced to 90% level (10% reduction) in post peak curve, and $\mu\delta$ (0.8) correspond to reduction of lateral load till 80% level (20% reduction) of V_{max}

Table 2:- Summary of present results and their comparison with previous similar studies

Author	ID	Size	f _c	P/P ₀	Øh	S	ρ _{sh}	V _{max}	M _{max}	μδ(0.9)	μδ(0.8)	μσ(0.9)	μσ(0.8)	E(t)
Present Study	D1	300x300	32.74	0.35	10	75	1.31	100.5	209.98	2.93	-	7.82 ^(0.95)	-	56982.41
	UC1	300x300	32.34	0.35	10	300	0.33	87.72	171.08	1.7	1.9	4.11	4.71	19939.25
	UC2	300x300	33.40	0.35	10	300	0.22	89.10	159.66	1.7	1.9	2.5	3.07	16893.2
Sheikh et al. 1993	AS19	305x305	32.27	0.39	10	107.6	1.3	121.7	202.1	-	4	10	19	1230
Lacobucchi et al. 2003	AS1NS	305x305	31.4	0.33	10	300	0.61	108.2	180.4	-	3.7	4.1	5.3	66200
	AS7NS	305x305	37.0	0.33	10	300	0.61	117.2	208.4	-	-	-	-	7700
Meta et al. 2014	UC	300x300	16	0.22*	8	300	-	63	106.5	-	-	-	-	-
Yang, 2016	ZZ1	210x210	46.4	0.18	6	90	-	46.5	-	-	7.44	-	-	-
Mo et al. 2000	C1-1	400X400	24.94	0.11*	6.4	50	-	250	-	-	5.50	-	-	344675.2
	C1-2	400X400	26.67	0.16*	6.4	50	-	264.53	-	-	5.38	-	-	463477
	C1-3	400X400	26.13	0.22*	6.4	50	-	305.30	-	-	5.26	-	-	471402.8
	C2-1	400X400	25.33	0.11*	6.4	52	-	243.29	-	-	5.78	-	-	472665.3
	C2-2	400X400	27.12	0.16*	6.4	52	-	273.07	-	-	5.65	-	-	515284.9
	C2-3	400X400	26.77	0.21*	6.4	52	-	304.44	-	-	5.35	-	-	473566.4
Aquino et al. [33]	6	D=500	32	-	10	200		165						
Li et al [34]	A0	200x200	44.8	0.35	8	100		190.87			3.57			
Ying Ma et. al. [28]	C0-40	D=260	32.4	0.40	8	100		75.84			5.82			
Guo et al. [35]	S1	600x250	42.9	0.10	8	60		64.8			>4.57			

Note: - (1). 0.9 signifies 90% level (10% reduction) of maximum value in post peak curve. (2). 0.8 signifies 80% level (10% reduction) of maximum value in post peak curve.

CONCLUSIONS

The main aim of this study was to examine the seismic performance of under confined reinforced concrete columns designed before the ductile detailing codes were implemented. It is believed that this effort would enable designing suitable retrofit for these deficient columns. Towards this end, full scale stubbed square RC columns representing two under-confined columns and one reference well confined column were cast and tested. A large amount of response seismic data was collected to enable quantification of deficit in under-confined columns. Following conclusions can be drawn from this study:

- A maximum reduction (attained at 3.5% drift) in lateral load capacity by 13% and in moment capacity by 24% was recorded in under-confined columns as compared to reference well confined column designed according to the current code requirements. This significantly inferior response of under confined specimens despite having similar cross section indicated the adverse effects of higher tie spacing on the lateral load capacity. This observation also signifies that, inferior confinement due to larger spacing of tie allowed dilation of core concrete at higher drift levels (>2%) which ultimately resulted to inferior flexural stresses.

- A reduction in axial load carrying capacity in under-confined columns is 17% and 40% for specimens UC1 and UC2 respectively at 5% drift indicate incapability of these RC columns in maintaining the axial gravity loads during earthquake.
- Displacement ductility factor of 1.9 noted in the under confined columns was 52.5% lower than the desired value of 4 and Curvature ductility factors were 76.45% and 84.65% lower than the desired values of 20 in the deficient columns. Other key deformability and energy dissipation parameters also indicate poor performance of under confined concrete columns.
- This study highlights significantly lower values of structural performance indices in reinforced concrete columns designed according to the pre ductile detailing code era typical in many existing structures in seismically active areas of India and thus are in dire need of retrofitting to match current structural performance indices.

NOTATIONS

P_0 – Theoretical axial capacity of column under concentric axial load.

f'_c – Compressive strength of concrete cylinder ($\phi=100\text{mm}$ and $L=200\text{mm}$).

A_g – Gross area of column, A_c – Net area of concrete.

f_y – Yield strength of longitudinal reinforcement.

A_{st} – Area of longitudinal reinforcement.

A_b – Effective area of lateral reinforcement bar.

$A_{sh(\text{req})}$ – Area of one hoop/stirrup required.

$A_{sh(\text{Provided})}$ – Area of one hoop/stirrup provided.

ρ_{sh} – Transverse reinforcement ratio.

s – Spacing of transverse reinforcement c/c.

ϕ_h – Diameter of transverse reinforcement.

b_c – Leg distance of stirrup.

λ – Drift ratio.

δ – Lateral deflection.

δ' – Deflection of LVDTs at different locations.

Δ – Tip deflection of the column.

$\delta_{y(t)}$ – Theoretical yield deflection of cracked section.

λ_y – Yield drift ratio.

V – Lateral load.

P – Axial load.

M – Moment.

ϕ – Curvature.

θ – Flexural rotation

S_1 – Segment Length.

h_t – Span between LVDTs.

K_n – Stiffness of n^{th} cycle.

E_n – Energy dissipation capacity in n^{th} cycle.

μ_ϕ – Curvature ductility factor, and μ_δ – Displacement ductility factor.

BIBLIOGRAPHY

- [1] T. Ohno and T. Nishioka, "An experimental study on energy absorption capacity of columns in reinforced concrete structures," *Proceedings of the JSCE, Structural Eng./Earthquake Eng.*, vol. 1, no. 2. pp. 23–33, 1984.
- [2] R. D. Iacobucci, S. A. Sheikh, and O. Bayrak, "Retrofit of Square Concrete Columns with Carbon Fiber-Reinforced Polymer for Seismic Resistance," *ACI Struct. J.*, vol. 100, no. 6, pp. 785–794, 2003.
- [3] IS-13920:2016, "Ductile Design and Detailing of Reinforced Concrete Structures Subjected to Seismic Forces- Code of Practice (First Revision)," no. July, 2016.
- [4] ACI:318-11, "Building Code Requirements for Structural Concrete and Commentary," *Am. Concr. Inst.*
- [5] (CSA)A23.3-04, *Design of concrete structures (CSA)*. .
- [6] NZS-3101:2006(Part-I), *Concrete structures standard - The design of concrete structures*, vol. 1. 2006.
- [7] S. Jain and N. Nigam, "Historical developments and current status of earthquake engineering in India," *Proc. 12th world Conf. ...*, pp. 1–8, 2000.
- [8] A. C. I. Committee, "Guide for Testing Reinforced Concrete Structural Elements under Slowly Applied Simulated Seismic Loads," 2013.
- [9] S. a Sheikh, "A Comparative Study of Confinement Models," *ACI Journal*, vol. 79, no. July-August. pp. 296–306, 1982.
- [10] H. Aoyama, "Moment-Curvature Characteristics of Reinforced Concrete Members Subjected to Axial Load and Reversal of Bending," 1964.
- [11] M. Saatcioglu and G. Ozcebe, "Response of reinforced concrete columns to simulated seismic loading," *ACI Struct. J.*, vol. 86, no. 1, pp. 3–12, 1989.
- [12] S. a. Sheikh and S. S. Khoury, "Confined concrete columns with stubs," *ACI Structural Journal*, vol. 90. pp. 414–414, 1993.

- [13] S. a Sheikh, D. V Shah, and S. S. Khoury, "Confinement of High Strength Concrete Column.Pdf," *ACI Structural Journal*, vol. 91, pp. 100–111, 1994.
- [14] a Azizinamini and W. Corley, "effect of transverse reinforcement on seismic performance of columns.PDF," *Aci Struct. J.*, no. 89, 1992.
- [15] Y. L. Mo and S. J. Wang, "Seismic Behavior of RC Columns With Various Tie Configuration," *J. Struct. Eng.*, vol. 5, no. 3, pp. 1122–1130, 2000.
- [16] H. Kang Ning Li, "Reinforced concrete columns under varying axial load and bi-directional lateral load reversals.pdf." 1988.
- [17] S. A. Sheikh and Y. Li, "Design of FRP confinement for square concrete columns," *Eng. Struct.*, vol. 29, no. 6, pp. 1074–1083, 2007.
- [18] ACI 440, *Guide for the design and construction of externally bonded FRP systems for strengthening concrete structures*, vol. 24. 2017.
- [19] IS 456:2000, "Plain and Reinforced Concrete - Code of practice," *Bur. Indian Stand.*, no. July, 2000.
- [20] IS-13920:1993, "DUCTILE DETAILING OF REINFORCED CONCRETE STRUCTURES SUBJECTED TO SEISMIC FORCES — CODE OF PRACTICE," *Bur. Indian Stand.*, vol. 1993, no. Reaffirmed 1998, 2002.
- [21] IS 10262: 2009, *Indian concrete mix design guide lines*. 2009.
- [22] D. Kato, L. I. Zhuzhen, K. Suga, and Y. Nakamura, "Effects of Reinforcing Details on Axial Load Capacity of R/C Columns," *13th World Conf. Earthq. Eng.*, no. 337, p. 11, 2004.
- [23] M. S. Memon and S. A. Sheikh, "Seismic Resistance of Square Concrete Columns Retrofitted with Glass Fiber-Reinforced Polymer," *ACI Struct. J.*, vol. 102, no. 5, pp. 774–783, 2005.
- [24] K. Elwood and J. Moehle, "Evaluation of existing reinforced concrete columns," *13th World Conf. Earthq. Eng.*, no. 579, 2004.
- [25] G. Lin, Z. Hu, S. Xiao, and J. Li, "Axial Collapese of Reinforced Concrete Columns," in

- 13 th World Conference on Earthquake Engineering DAMS*, 2004, no. 1085.
- [26] T. Nakamura and M. Yoshimura, “Gravity Load Collapse of Reinforced Concrete Frames,” *CE 299 Rep. Univ. California, Berkeley*, pp. 1–11, 2014.
- [27] C. T. N. Tran, “Experimental and Analytical Studies on the Seismic Behavior of Reinforced Concrete Columns With Light Transverse Reinforcement,” *PhD Thesis*, vol. 4014126, no. 11, pp. 1–11, 2010.
- [28] Y. Ma, Y. Che, and J. Gong, “Behavior of corrosion damaged circular reinforced concrete columns under cyclic loading,” *Constr. Build. Mater.*, vol. 29, pp. 548–556, 2012.
- [29] H. Saadatmanesh, M. R. Ehsani, and L. Jin, “Repair of earthquake-damaged RC columns with FRP wraps,” *ACI Struct. J.*, vol. 94, no. 2, p. 206–X, 1997.
- [30] C. G. Bailey and M. Yaqub, “Seismic strengthening of shear critical post-heated circular concrete columns wrapped with FRP composite jackets,” *Compos. Struct.*, vol. 94, no. 3, pp. 851–864, 2012.
- [31] B. Li and R. Park, “Confining Reinforcement for High-Strength Concrete Columns,” 2004.
- [32] X. Zhu, T. Sato, W. Jiang, a Ono, and Y. Shimuzu, “Behavior of Reinforced Concrete Column Under High Axial Load,” *Proc. 9th World Conf on Earthquake Engineering*. pp. 353–358, 1988.
- [33] W. Aquino and N. M. Hawkins, “Seismic Retrofitting of Corroded Reinforced Concrete Columns Using Carbon Composites,” *ACI Struct. J.*, vol. 104, no. 3, pp. 348–356, 2007.
- [34] J. Li, J. Gong, and L. Wang, “Seismic behavior of corrosion-damaged reinforced concrete columns strengthened using combined carbon fiber-reinforced polymer and steel jacket,” *Constr. Build. Mater.*, vol. 23, no. 7, pp. 2653–2663, 2009.
- [35] A. Guo, H. Li, X. Ba, X. Guan, and H. Li, “Experimental investigation on the cyclic performance of reinforced concrete piers with chloride-induced corrosion in marine environment,” *Eng. Struct.*, vol. 105, pp. 1–11, 2015.